Deltares

Study on low frequency wave penetration in SWAN

Validation of DCTA method

Study on low frequency wave penetration in SWAN
Validation of DCTA method

Author(s)
Madelief Doeleman
Jacco Groeneweg

Study on low frequency wave penetration in SWAN
Validation of DCTA method

Client	Rijkswaterstaat Water, Verkeer en Leefomgeving
Contact	de heer R. Vos
Reference	WK01 2021 Plan van Aanpak Kennis voor Keringen, version 4.2 Plan van Aanpak KP Zeespiegelstijging SWAN verbeteringen, versie 0.6
Keywords	Wave modelling, SWAN, triad interactions, wave penetration, DCTA

Document control	
Version	1.2
Date	05-04-2024
Project nr.	11208057-017
Document ID	11208057-017-GEO-0003
Pages	39
Classification	
Status	final

Author(s)		
	M.W. Doeleman	
	J. Groeneweg	

The allowed use of this table is limited to check the correct order-performance by Deltares. Any other client-internal-use and any external distribution is not allowed.

Doc. version	Author	Reviewer	Approver
1.2	M.W. Doeleman J. Groeneweg	J. van Nieuwkoop	P. van Steeg

Summary

Within the Sea Level Rise Knowledge Program (“Kennisprogramma Zeespiegelstijging” KP-ZSS), coastal safety assessments are performed to assess the effect of sea level rise of +0.5 m till +5 m on the failure probability of dike segments along the Dutch coast. Use is made of the SWAN model, which is known to underestimate the penetration of North Sea waves into the Wadden Sea towards the coast of Frisia and Groningen. Two potential improvements were considered at the start of this program: inclusion of Bragg scattering and a new three-wave interaction method called DCTA. The DCTA method is able to transfer energy to the low frequency part of the spectrum as well, in contrast to the default LTA method. The focus in this report is on the latter one. The objective of this study is to validate the DCTA method for triad modelling against SWASH results, 2D laboratory measurements (Taman case) and field cases (Eastern Wadden Sea) to see whether its present implementation in SWAN could lead to an improvement of the penetration of low-frequency waves from the North Sea into the Wadden Sea.

Apart from comparing the SWAN results with measurements and SWASH results at various measurement locations, also the evolution along rays of both variance density spectra and triad source terms has been analyzed. For the situation without wind and currents a comparison with SWASH results has been made. Various settings for both the original LTA method and the newly developed DCTA method have been considered. For the DCTA method both the collinear and non-collinear version have been considered. Like the LTA method, in the collinear DCTA method only triads in the same directions are accounted for. In the non-collinear version the interaction between waves from different directions are also considered.

From the analyses we conclude that, from a qualitative point of view, the DCTA method seems to be an improvement over the LTA method. The DCTA method transfers energy to lower frequencies, whereas the LTA method does not. In addition, the shape of the DCTA source term is more realistic, in some cases LTA leads to physically unrealistic peaks in the spectrum. For the Taman case the variance density computed with the DCTA method at the low frequencies and at the first harmonic does not compare to what is measured or computed with SWASH. The variance density at these frequencies can be increased by decreasing the default value for the critical Ursell number or increasing the scaling factor significantly.

For both the laboratory case and the field case wave energy is accumulated near the channel edge in the SWAN computations, but also in the SWASH computations, at least for the field case. The wave energy strongly decreases when crossing the channel edge towards the deeper part and underestimates the wave energy at the measurement locations close to the coast. Since SWAN and SWASH show a similar behavior, another yet unknown mechanism seems to be responsible for the underestimation of the low-frequency energy at the measurement locations near the Groningen and Frisian coast. It is strongly recommended to investigate what other mechanism this could be.

For the Eastern Wadden Sea case, the DCTA collinear method is as fast as the LTA method per iteration. The computational time of the non-collinear version of the DCTA method is 60 times longer than the collinear version. Therefore, the non-collinear version of the DCTA method is not appropriate for practical (BOI and operational) applications.

Since for some cases the LTA method leads to unrealistic shapes of the variance density spectra, whereas the DCTA method does not, the DCTA method is recommended over the LTA method for application in future studies. Although HKV (2022) concluded that the DCTA

method is sensitive for the choice of the scaling parameter λ and critical Ursell number, this could not be confirmed in this study. Nevertheless, we recommend to explore the sensitivity for these parameters for a wide range of tests. If the sensitivity appears to be significant, reconsider the DCTA method and underlying assumptions (e.g. bi-phase formulation) in general and the scaling parameter in particular. If the sensitivity is not large, it is recommended to calibrate the DCTA method together with a breaker model, again using a wide range of tests. Finally, since the non-collinear version of the DCTA method does not appear to be energy conserving, a close look at its implementation should be considered.

Samenvatting

Binnen het Kennisprogramma Zeespiegelstijging (afgekort KP-ZSS) wordt het effect van zeespiegelstijging van +0.5 m tot 5 m op de veiligheid tegen overstromen van de kustgebieden onderzocht. Daarbij wordt onder andere gebruik gemaakt van de spectrale golfmodel SWAN. We weten van dit model dat het de doordringing van lange golven afkomstig van de Noordzee in de Waddenzee naar de Friese en Groningse kust onderschat. Twee mogelijke verbeteringen zijn beschouwd bij de start van het programma: inbedding in SWAN van Bragg scattering en een nieuw model (DCTA) voor drie-golf wisselwerkingen. In tegenstelling tot de LTA methode, vindt er bij de DCTA methode niet alleen energie overdracht naar hogere frequenties plaats maar tevens naar lagere frequenties. De focus van dit rapport is op het laatste. Het doel van deze studie is om de DCTA methode te valideren met behulp van SWASH resultaten en metingen van een 2D laboratorium case (Taman) en een veldcase (Oostelijke Waddenzee) om na te gaan of de huidige implementatie van de DCTA methode in SWAN leidt tot een verbetering van de doordringing van laag-frequente energie de Waddenzee in.

Naast het vergelijken van SWAN resultaten met metingen en SWASH resultaten op diverse meetlocaties, analyseren we ook de evolutie van variantiedichtheidsspectra en triad brontermen langs een aantal raaien. Voor de situatie zonder wind en stroming is een vergelijking met SWASH resultaten gemaakt. Verschillende instellingen voor de oorspronkelijke LTA methode en de nieuw ontwikkelde DCTA methode zijn beschouwd. Voor de DCTA zijn zowel de collineaire als de niet-collineare versies bekeken. Net als voor de LTA methode beschouwt de DCTA collineaire methode alleen triads in dezelfde richting. In de niet-collineaire versie wordt de interactie tussen golfcomponenten uit verschillende richting ook beschouwd.

Op basis van de uitgevoerde analyse concluderen we dat, vanuit kwalitatief oogpunt, de DCTA methode een verbetering is ten opzichte van de LTA methode. De DCTA methode verplaatst energie naar lage frequenties, waar de LTA dat niet doet. De vorm van de DCTA bronterm ziet er realistischer uit, in een aantal gevallen leidt de LTA methode tot onrealistische pieken in het spectrum. Kwantitatief zijn er nog wel aanmerkingen. Voor de Taman case onderschat SWAN met DCTA de variantie dichtheid in het lage frequentiebereik en rondom de eerste harmonische, zoals enerzijds gemeten en anderzijds berekend met SWASH. De variantie dichtheid bij genoemde frequentiebereiken neemt toe wanneer de default waarde van het kritisch Ursell getal wordt verlaagd of de schalingsfactor significant wordt verhoogd.

Voor zowel de laboratorium case als de veld case hoopt de golfenergie in de SWAN berekeningen zich op langs de rand van de geul. Dit is ook in sterke mate het geval in de SWASH berekeningen, voor de Taman case lijkt dit minder het geval. De golfenergie neemt sterk af in de geulen en onderschat de gemeten (met name laag-frequente) golfenergie uiteindelijk op de meetlocaties vlakbij de kust. Omdat SWAN en SWASH hierin vergelijkbaar gedrag vertonen lijkt het er sterk op dat een ander, vooralsnog onbekendmechanisme verantwoordelijk is voor de onderschatting van de laag-frequente energie op de meetlocaties voor de kust van Friesland en Groningen. Het wordt sterk aanbevolen om te onderzoeken welk(e) mechanisme(n) dit zou(den) kunnen zijn.

Voor de Oostelijke Waddenzee case is de collineare versie van de DCTA ongeveer even snel als de LTA methode per iteratie. De rekentijd met de niet-collineaire versie van de DCTA is echter 60 keer langer dan met de collineaire versie. Daarom is de niet-collineaire versie nog niet geschikt voor praktische (BOI en operationele) toepassingen.

Omdat de LTA methode voor een aantal cases tot onrealistische vormen van de energiedichtheidsspectra leidt, waar de DCTA methode dat niet doet, bevelen we aan de DCTA methode te gebruiken in plaats van de LTA methode. Ondanks dat HKV (2022) heeft laten zien dat de DCTA methode gevoelig is voor de keuze van de schalingsparameter λ en het kritisch Ursell getal, is dat in deze studie niet bevestigd. Desondanks bevelen we ten zeerste aan om de gevoeligheid van deze parameters te onderzoeken voor een brede testset. Mocht deze gevoeligheid groot zijn, heroverweeg dan de DCTA methode en onderliggende aannames (bijvoorbeeld de formulering van de bifase) in het algemeen en de formulering van de schalingsparameter in het bijzonder. Wanneer de gevoeligheid klein is kalibreer dan de DCTA methode tezamen met een van de brekermodellen, waarbij opnieuw een brede testset wordt gebruikt. Tenslotte wordt aanbevolen de implementatie van de niet-collineaire versie van de DCTA methode nog eens goed te controleren, omdat deze methode niet energiebehoudend lijkt te zijn.

Contents

1 Introduction

1.1 Background

Within the Sea Level Rise Knowledge Program (“Kennisprogramma Zeespiegelstijging” KP-ZSS), coastal safety assessments are performed to assess the effect of sea level rise of +0.5 m till +5 m on the failure probability of dike segments along the Dutch coast. The database that is used for these assessments consists of wave conditions determined with the SWAN (Simulating Waves Nearshore) wave model. Previous research (e.g. Alkyon, 2009) has shown that SWAN underestimates the penetration of low frequency waves from the North Sea towards the Frisian and Groningen dikes. This impacts calculation of wave run-up and overtopping. At the time, a non-physics based refraction-limiter has been used to improve the low frequency penetration (Deltares, 2009).

Over the last couple of years various changes to SWAN have been made (for a summary see the Release Notes on https://swanmodel.sourceforge.io/), some of them within the Program Knowledge for Flood Defences (“Kennis voor Keringen”). None of those led to improvements related to the underestimation of low-frequency wave penetration, which are necessary for a proper coastal safety assessment in complex Dutch estuaries: Wadden Sea, Western Scheldt and Eastern Scheldt. Within the Sea Level Knowledge Program two potential improvements were considered: inclusion of Bragg scattering and a new three-wave interaction method called DCTA. The overarching project is structured as shown in Figure 1.1. This report will address the in yellow highlighted SWAN validation phase.

The development of a Bragg scattering source term and its implementation in SWAN has been described in Rijnsdorp et al. (2021), as well as the verification and validation of the source term. They concluded that Bragg scattering does not contribute to wave transmission across tidal channels. The focus of the present report is on the DCTA method to model three wave interactions in shallow water.

The DCTA method was developed by Booij et al. (2009). Within the present project significant improvements to the DCTA code has been made, reported in HKV (2022). Important phenomena are the evaluation of both sum and difference interactions as well as collinear and non-collinear interactions. Apart from that also the transformation to an equilibrium shape of the spectrum due to sub- and super-harmonic interactions is important. By applying a prototype (Matlab code) of the adapted formulation in isolation, so without other physical processes, it has clearly been shown that the desired phenomena are represented over a horizontal bed. In HKV (2022) three laboratory cases were considered for verification purposes: the 1DH cases by Smith (2004) and Beji and Battjes (1993) and the 2DH cases by Nwogu (1994). The results obtained with the prototype model agreed with the measurements in a qualitative way. Due to the absence of various physical mechanisms in the prototype model, a quantitative agreement is not yet obtained. Optimal values for the wave breaker parameter and the scaling coefficient of the DCTA show a lot of spreading. Quantitative improvements are to be expected after implementation in SWAN and extensive model calibration, since various limitations of the simplified energy model in the prototype model do not account for SWAN. HKV (2022) recommends to consider a more extensive measurement set. The variation in bed formations is limited.

The DCTA method in the prototype model formed the basis for the implementation in SWAN version 41.45 (SWAN team, 2023). The formulation has been calibrated on 1D laboratory cases of Boers (1996) and Beji and Battjes (1994), resulting in a specific scaling coefficient.

Further validation according to the testcases of Delilah, Haringvliet, Ameland Inlet, Eastern Scheldt and Western Scheldt led to the conclusion that the DCTA method is more stable than the LTA formulation (Eldeberky and Battjes, 1995), being one of the reasons to make the (collinear version of the) DCTA method the default method to model triads in SWAN.

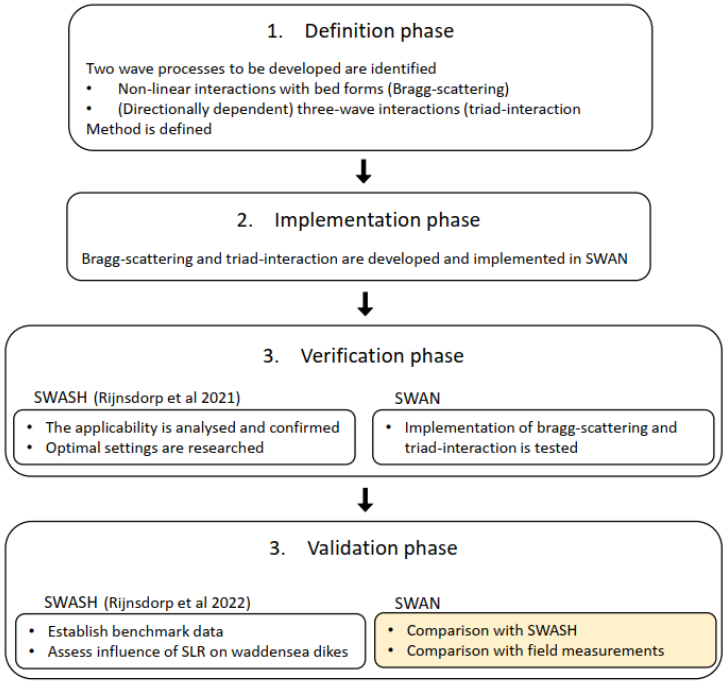

Figure 1.1: Structure of the overall KP-ZZS low frequency wave energy project. This report elaborates on the in yellow highlighted SWAN validation phase.

1.2 Objectives

The objective of this report is to validate the DCTA method for triad modelling against SWASH results and measurements in 2D laboratory and field cases and find out whether its present implementation in SWAN could lead to an improvement of the penetration of low-frequency waves from the North Sea into the Wadden Sea.

1.3 Approach

Various settings of both the LTA as well as the DCTA method are considered for different cases. The cases include the laboratory case for Taman (Groeneweg et al., 2015) and the Eastern Wadden Sea. For the Taman case a comparison is made with measurements as well as SWASH results (Rijnsdorp et al., 2021). The Eastern Wadden Sea case includes the Frisian and Lauwers Inlet and is based on the storm of 8/9 November 2007. The results for this case are compared with SWASH (without wind and currents only at the Frisian and Lauwers Inlet) and with measurements (with winds and currents). In all cases also the evolution of variance density spectra and source terms has been analyzed.

In Chapter 2 both the LTA and the DCTA methods are described. The laboratory tests of Taman and the Wadden Sea case are outlined in Section 3.1. In Section 3.2 the SWAN settings as well as the triad variations considered are described. The analysis of the SWAN results, including the comparison with both SWASH results and measurements, is elaborated in Chapter 4. Finally, conclusions and recommendations are given in Chapter 5.

1.4 Team

The validation of the DCTA method has been carried out by Madelief Doeleman and Jacco Groeneweg (Deltares). Results have been discussed with Marcel Zijlema (Delft University) and Matthijs Benit (HKV). The report has been reviewed by Joana van Nieuwkoop (Deltares) and Robert Vos (Rijkswaterstaat – WVL).

2 Methods for three wave interactions

With SWAN version 41.45 three methods are available to compute nonlinear interactions in finite water depth. The first method is the Lumped Triad Approximation (LTA) method, developed by Eldeberky (1996). The second method is the Stochastic Parametric model based on Boussinesq equations (SPB) method by Becq-Girard et al. (1999). The third method is the Distributed Collinear Triad Approximation (DCTA) of Booij et al. (2009). The LTA and DCTA methods are considered in this study and described in Section 2.1 and 2.2. Both methods use a parametrization of the biphase. This is described in Section 2.3.

2.1 The LTA method

The LTA method of Eldeberky (1996) is given by

$$S_{nl3}(\sigma) = S^{+}_{nl3}(\sigma) + S^{-}_{nl3}(\sigma) \tag{2.1}$$

with

$$S^{+}_{nl3}(\sigma) = \max\left[0, \alpha c_{\sigma} c_{g,\sigma} J^2 \sin(-\beta)\{E^2(\sigma/2) - 2E(\sigma/2)E(\sigma)\}\right] \tag{2.2}$$

and

$$S^{-}_{nl3}(\sigma) = -2S^{+}_{nl3}(2\sigma) \tag{2.3}$$

Eq. (2.2) represents a positive contribution of the self interaction at frequency $\sigma/2$ contributing to the energy at σ. Eq. (2.3) represents a negative contribution of the self interaction at frequency σ (taking away from $E(\sigma)$). This means that only self interactions are considered and energy is transferred from frequency σ to 2σ.

The so-called OCA implementation (Original Collinear Approximation) of the LTA is applied in this study. The parameters used in these equations denote:

σ	radian frequency
α	proportionality coefficient (default: set here at 0.1)
c_{σ}	phase velocity at σ
$c_{g,\sigma}$	group velocity at σ
β	biphase of self-self interaction (see Section 2.3)
J	interaction coefficient

The interaction coefficient J is defined as

$$J = \frac{k^2_{\sigma/2}\left(gd + 2c^2_{\sigma/2}\right)}{k_{\sigma} d\left(gd + \frac{2}{15} g d^3 k^2_{\sigma} - \frac{2}{5}\sigma^2 d^2\right)} \tag{2.4}$$

with:

k_{σ}	wave number at σ
d	water depth
g	gravity acceleration

2.2 DCTA method

The DCTA method has been described in HKV (2022) and has been reformulated to be implemented in SWAN (SWAN team, 2023). Here we present the energy-flux conservative expression, that has been implemented in SWAN.

$$S_{nl3}(\sigma_1,\theta_1) = \lambda c_{g,1}\frac{\sin(-\beta)\tilde{k}^{2-p}}{\tilde{\sigma}^2 d^2}\,\mathrm{x}$$
$$\int_0^{2\pi}\int_0^{\infty}\left(\frac{\tanh\bar{k}d}{\bar{k}d}\right)^4\left(\frac{G(\Delta\theta_{23})}{G(0)}\right)^2 E(\sigma_3,\theta_3)\left[c_{g,2}k_2^p E(\sigma_2,\theta_2) - c_{g,1}k_1^p E(\sigma_1,\theta_1)\right]d\sigma_2 d\theta_2 \quad (2.5)$$

with $G(\Delta\theta_{23})$ the transfer function of Sand (1982) and $\Delta\theta_{nm} = \theta_n - \theta_m$. Eq. (2.5) is the non-collinear version. In the collinear version only wave components in direction θ_1 are considered, so $\theta_1 = \theta_2 = \theta_3$. The other parameters in Eq. (2.5) denote:

λ	scaling parameter (default: 4.4)
$\tilde{\sigma}$	mean frequency: m_1/m_0 with m_i the i-th spectral moment
$\tilde{k} = \tilde{\sigma}/\sqrt{gd}$	mean wave number
p	shape coefficient to force high frequency tail (default: 4/3)
$\bar{k} = (k_1 + k_2 + k_3)/3$	characteristic wave number of triad

2.3 Biphase parametrization

Both the LTA and the DCTA method use the biphase of the self-self interaction of the spectral peak β. Eldeberky (1996) proposed the following parameterization

$$\beta = -\frac{\pi}{2} + \frac{\pi}{2}\tanh\left(\frac{U_{r,crit}}{U_r}\right) \quad (2.6)$$

with $U_{r,crit}$ a tunable coefficient, called the critical Ursell number. The spectral Ursell number is defined as

$$U_r = \frac{gH_{m0}}{8\sqrt{2}}\left(\frac{T_{m01}}{\pi d}\right)^2 \quad (2.7)$$

where H_{m0} is the significant wave height and T_{m01} the mean wave period.

The critical Ursell number has been taken equal to 0.2 for a long time, as proposed by Eldeberky and Battjes (1995), based on a laboratory experiment. Zijlema (2023) notes that $U_{r,crit}$ = 0.2 sometimes leads to instabilities in the triad computations, especially with the LTA method. He recommends to follow the suggestion of Doering and Bowen (1995) to use a value of $U_{r,crit}$ = 0.63. In version 41.45 the default value for $U_{r,crit}$ has been changed from 0.2 to 0.63 (background of this choice is described in Zijlema (2023).

3 Description of test cases

3.1 Testcases

Two test cases are considered. The first is a laboratory case for a harbor entrance, described in detail in Groeneweg et al. (2015). Secondly the storm of 8/9 November 2007 within the Wadden Sea. For both cases measurements as well as SWASH results are available.

3.1.1 2D laboratory test: Taman

The laboratory experiments for the harbor entrance of Taman have been described in Groeneweg et al. (2015). Out of the six laboratory tests one has been selected for the validation of the DCTA in this study, namely case T02. The wave board at x = 0 m (see Figure 3.1) produced the following wave conditions: significant wave height H_s = 0.082 m, peak period T_p = 1.87 s and directional spreading of 20 degrees, assuming a JONSWAP spectrum. The mean wave direction is perpendicular to the wave board. Four wave height meters (whm0x) and four GRSMs (whm9x) measure the wave conditions, the GRSMs also provide directional information. The position of the instruments and bathymetry is shown in Figure 3.1. The tests do not include currents and wind.

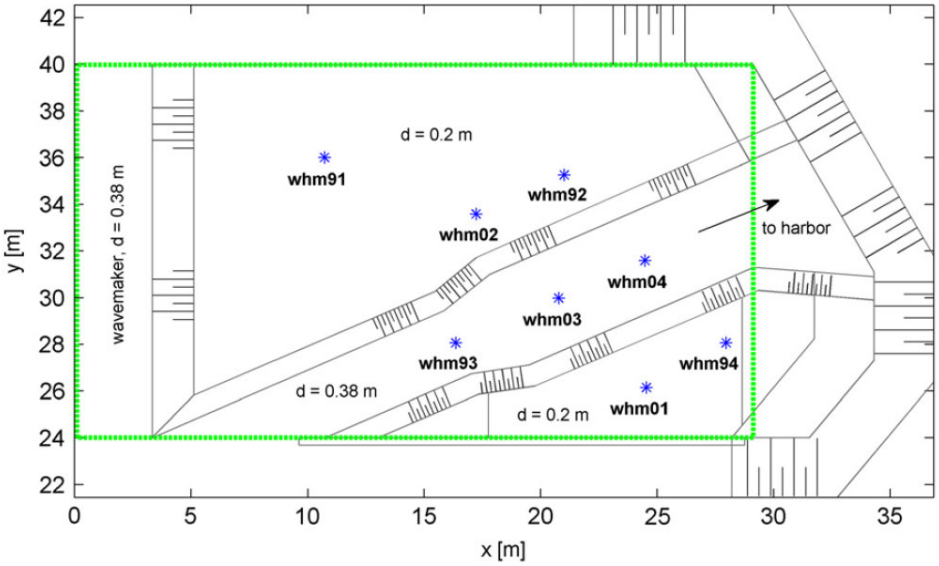

Figure 3.1: Layout of laboratory case of Taman (source: Groeneweg et al., 2015).

Rijnsdorp et al. (2021) set up a SWASH model for all six cases mentioned in Groeneweg et al. (2015). They compared their SWASH results to both measurements and SWAN version 41.31 results, in which the DCTA triad model was not yet implemented. The LTA model was used instead.

In the present study both laboratory measurements and SWASH results are used for comparison.

3.1.2 Field case: Eastern Wadden Sea

For the storm of 8/9 November 2007, measurements have been conducted at several locations, indicated in Figure 3.2. Most locations are close to the coast of Groningen and Frisia:

Wierumerwad (WRW), Pieterburenwad (PBW) and Uithuizerwad (UWH). In addition, Westereems Oost (WEO1) was used, which is located north-West of Borkum.

Figure 3.2 gives an overview of the Eastern Wadden Sea SWAN domain and measurement stations, retrieved from the SWIVT database (www.swivt.deltares.nl). For the white outlined Frisian and Lauwers Inlet SWASH computations are available. Therefore, these cut-out domains are also run in SWAN without currents and wind to be able to compare SWAN with the SWASH computations. In SWASH, currents and wind are not included.

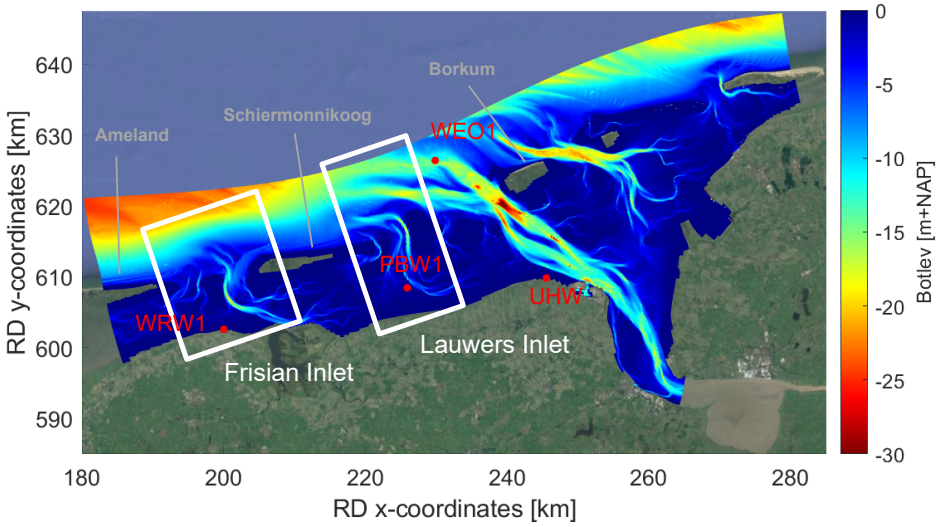

Figure 3.2: Measurement locations in the Eastern Wadden Sea: Wierumerwad (WRW), Pieterburenwad (PBW), and Uithuizerwad (UHW), and more offshore Westereems Oost (WEO1). The outlined Frisian Inlet and Lauwers Inlet indicate the SWASH domains.

3.1.2.1 Frisian and Lauwers inlet

For the Frisian and Lauwers Inlet SWAN computations have been carried out both with and without wind and currents, for one time instant being 9 November 2007, 9:40h. This is the instant with the largest wave height at UHW1, close to the instant of maximum water level (9:00h). This is Case F150ow07z008 in the SWIVT database. The wind speed is considered to be uniform over the SWAN domain, being 18.4 m/s with direction 298 °N. The water level and current varies over the domain. Also, the wave spectra at the offshore boundary are non-uniform.

For the situation without wind and current, the offshore boundary conditions are the same as imposed in the SWAN computations with wind and current. Comparison has been made with the SWASH computations described in Rijnsdorp et al. (2022). For the situation with wind and currents, a comparison with measurements at the locations WRW1 and PBW1 has been made. In both situations also the evolution of variance density spectra and the source terms for triads and depth-induced breaking over several rays has been analyzed. In both inlets two rays have been defined and presented in Figure 3.3. In the Frisian Inlet the northern ray (points 1-10) crosses the ebb-tidal delta and part of the tidal channel. The southern ray (points 11-WRW1) is perpendicular to the tidal channel and has WRW1 as end point. The northern and southern rays (points 23-29 and 30-PBW1 respectively) in the Lauwers Inlet have a north-south orientation and also cross the tidal channel. The northern ray crosses the tidal channel more or less perpendicular, the southern ray more or less parallel to the channel, having PBW1 as its end point.

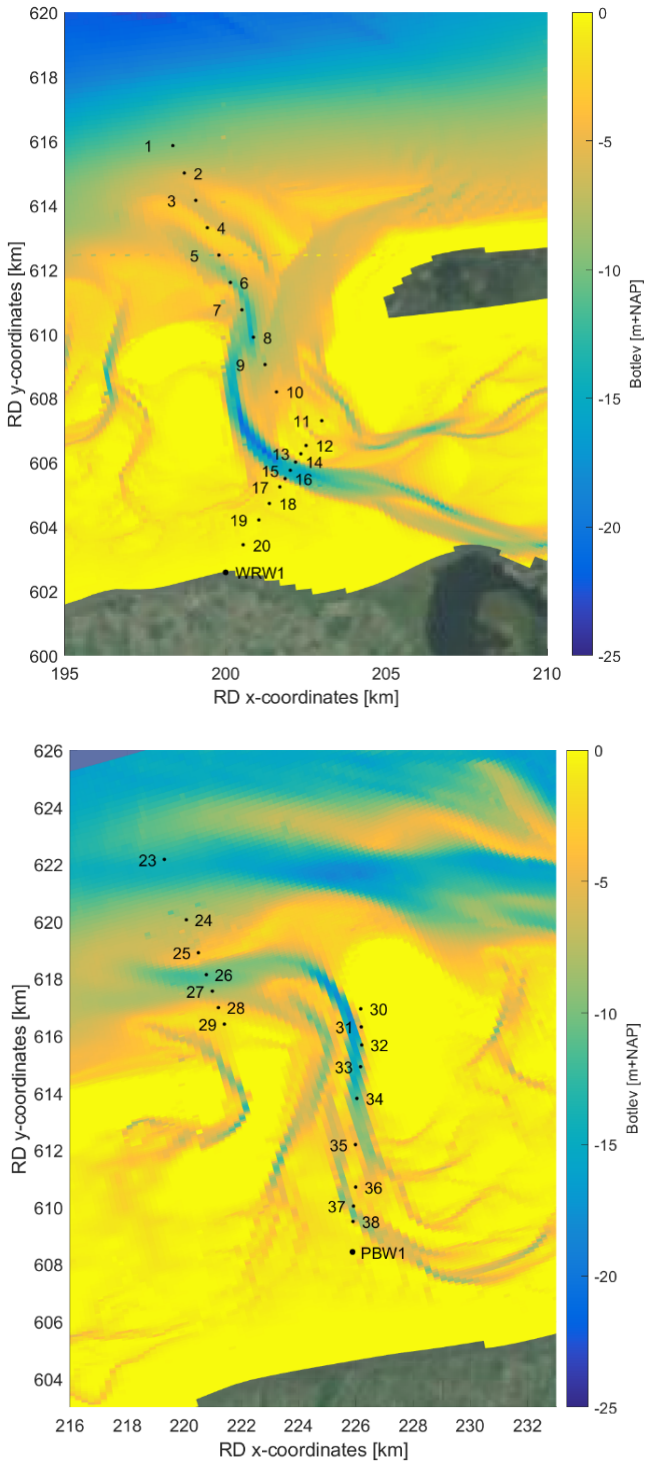

Figure 3.3: Rays of output locations in the Frisian Inlet (upper panel) and Lauwers Inlet (lower panel).

3.1.2.2 Uithuizerwad

For the whole domain of the Eastern Wadden Sea only a comparison with measurements has been made, using the same time instant as for the Frisian and Lauwers Inlet. In Figure 3.4 the

ray has been presented, over which the evolution of spectra and source terms has been analyzed. The end point of the ray is in UHW1, at which a comparison with measured wave data has been made. For this inlet no SWASH computations are available and therefore no comparison with SWASH could be made.

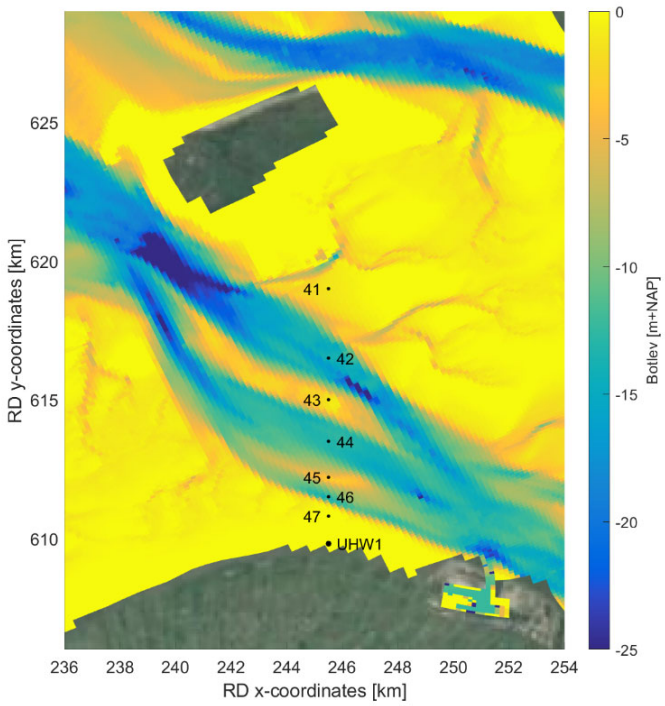

Figure 3.4: Rays of output locations in the Eastern Wadden Sea.

3.2 SWAN settings and variations

The SWAN computations have been carried out with version 41.45.2 at the Deltares Linux cluster. For a few cases SWAN version 41.45 from the SWAN website was used as for these computations SWAN was not yet available on the Deltares cluster. The results with both versions appeared identical.

For the cases with wind, the Komen et al. (1984) formulation for wind generation and whitecapping has been used and the DIA formulation for quadruplets. For the cases without wind, the quadruplets have been deactivated (`OFF QUAD`). Bottom friction has been modelled by the Jonswap formulation with friction parameter $C_{f,JON}$ = 0.038. The formulation by Battjes and Janssen (1978) has been applied to model depth-induced breaking.

```
GEN3 KOM
WCAP KOM cds2=2.36E-05 stpm=0.00302 powst=2 delta=0 powk=1
QUAD iquad=2 lambda=0.25 Cnl4=30000000 (with wind|no wind: OFF QUAD)
FRIC JONSWAP cfjon=0.038
BREA CON alpha=1 gamma=0.73
```

For triads both DCTA and LTA (OCA implementation) methods have been considered in this study, with the following settings:

DCTA: `TRIad DCTA trfac=4.4 p=1.33333 COLL|NONC  BIPH ELD urcrit=[urcrit]`

LTA: `TRIad itriad=11 trfac=0.1 cutfr=2.5 BIPH ELD urcrit=[urcrit]`

The Battjes-Janssen breaker formulation has been used because the DCTA has been calibrated with this breaker model (pers. comm. Marcel Zijlema). Note that using the Van der Westhuysen et al. (2007) formulations instead of the Komen et al. (1984) formulations for wind generation and whitecapping would probably not have led to different conclusions in this study.

The keywords within brackets indicate the variations being considered. The DCTA method can be run in two modes: collinear (`COLL`) and non-collinare (`NONC`) mode.. The keyword [urcrit] equals 0.63 (default) or 0.2 (used to be default in all previous SWAN versions) and denotes the critical Ursell number in the bi-phase formulation of Eldeberky (1995), see Eq. (2.6).

The variations being considered are indicated in Table 3-1.

Table 3-1: Settings for triad formulation, critical Ursell number and DCTA version (collinear/non-collinear)

Name	Triad form	[urcrit]	[colvar]
Base	DCTA	0.63	COLL
Nonc	DCTA	0.63	NONC
Ur	DCTA	0.2	COLL
OCA	LTA-OCA	0.63	-
OCA-Ur	LTA-OCA	0.2	-

For the laboratory case of Taman, case T02 the spatial resolution of the SWAN computations is 0.1 m, the frequency range is between 0.2 Hz and 3.0 Hz and the full circle of directions is divided in 36 sectors of 10 degrees. Both the spatial resolution and directional resolution has been halved to 0.05 m and 5 degrees respectively. This had no significant effect on the wave conditions at the measurement locations.

For the Eastern Wadden Sea case a frequency range between 0.03 Hz and 1.0 Hz has been used. The full circle with 36 sectors of 10 degrees has been considered.

4 Analysis of test results

4.1 Taman case

First of all we start with a reproduction of the case analyzed in Groeneweg et al. (2015) using the latest SWAN version 41.45. In the latter study the SWAN computations were carried out with the LTA method, using a critical Ursell number in the biphase parameterization (2.6) of 0.2. The comparison between the observed energy density spectra, and those computed by SWASH (Rijnsdorp et al., 2021) and SWAN, for Taman case T02, is shown in Figure 4.1.

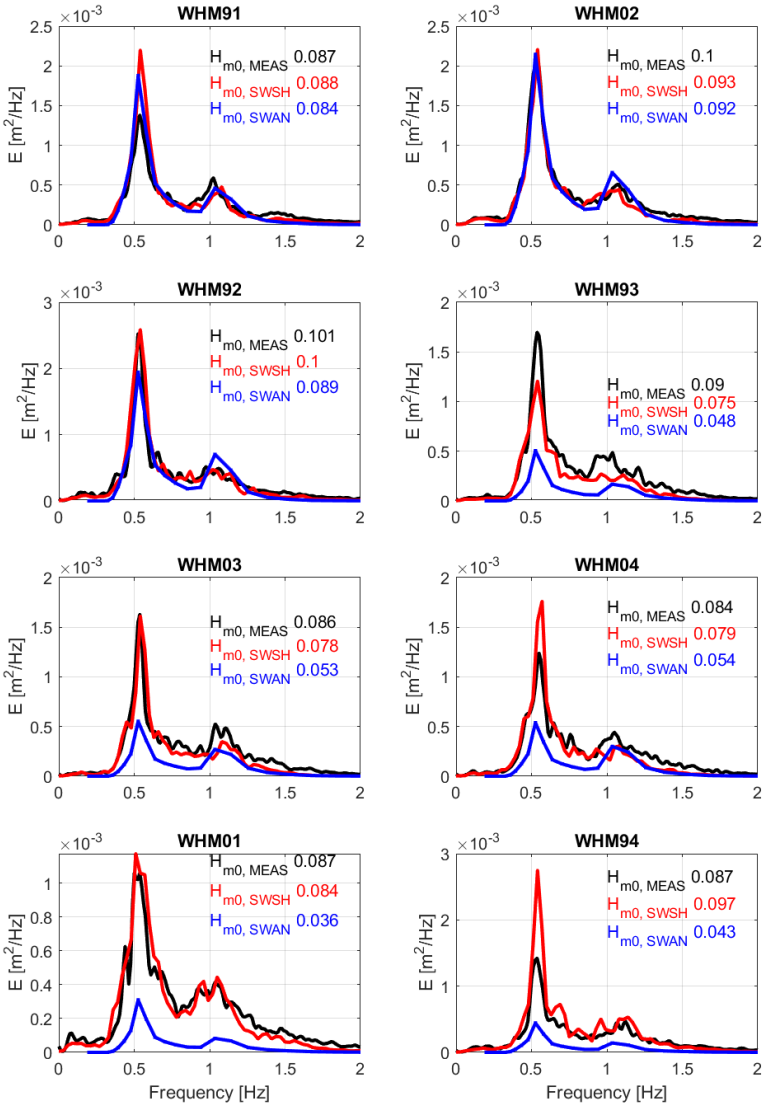

Figure 4.1: Variance density spectra for the Taman case T02 (from Groeneweg et al., 2015): observed (black), computed with SWASH (red) and with SWAN (blue). The LTA triad method (OCA implementation) in SWAN has been used with $U_{r,crit}$ = 0.2.

On the seaward side of the channel (WHM91, WHM02, WHM92) both SWAN and SWASH predict the observed energy density spectra reasonably well. The amount of energy at the first

harmonic is reproduced nicely. The energy transfer towards the low frequencies is modelled by SWASH, not by the LTA method in SWAN. The total amount of wave energy inside the channel (WHM93, WHM03, WHM04) is significantly underpredicted by SWAN. The difference between the measured significant wave height and the one computed with SWAN is almost a factor 2. The difference gets larger across the channel (WHM01 and WHM94). SWASH reproduces the observations very well. These conclusions are in line with those drawn in Groeneweg et al. (2015), although not SWASH but TRITON was used.

The next step is to consider the base case, see Table 3-1. The energy density spectra obtained with the DCTA formulation in SWAN have been compared with the measured and SWASH spectra, as can be seen in Figure 4.2. Though hard to see from the figure, some low-frequency energy has been generated with SWAN at the seaward locations (WHM91, WHM02, WHM92), but less than measured. At these locations also the energy at the first harmonic has been underestimated significantly. Inside and across the channel, significant underestimation of wave energy by SWAN can be observed. This is similar to the results using the LTA and a first indication that the underestimation is caused by a yet unknown mechanism (e.g. refraction) that depends on depth variations.

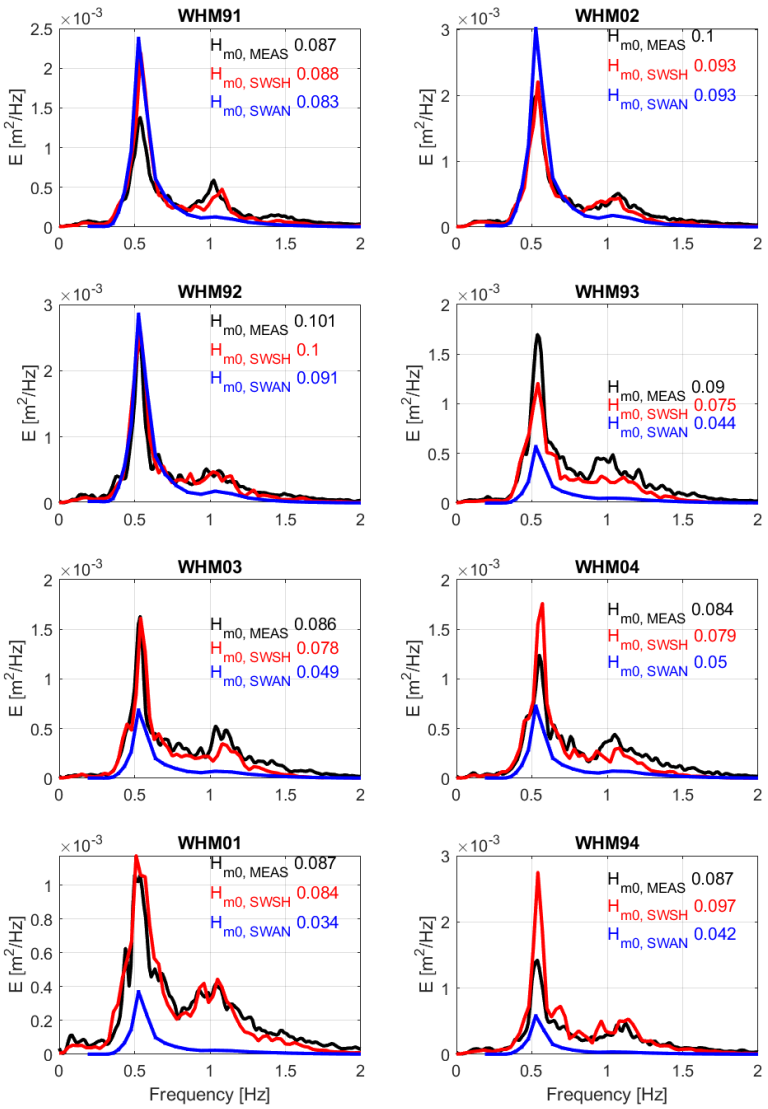

Figure 4.2: Variance density spectra for the Taman case T02: observed (black), computed with SWASH (red) and with SWAN (blue). The collinear version of the DCTA formulation in SWAN has been used with $U_{r,crit}$ = 0.63. This is the base case.

In Figure 4.3 the variance density spectra computed by SWAN for the variations mentioned in Section 3.1.1 (Table 3-1) have been presented, for the seaward location WHM92 and the channel location WHM04. The underestimation of wave energy inside the channel is more or less the same for all triad variations, even for the non-collinear DCTA version.

For WHM92, the original LTA method (with $U_{r,crit}$ = 0.2, magenta color) leads to an overestimation of the energy at the first harmonic. Increasing the critical Ursell number in the biphase formulation to 0.63 (cyan colored line) decreases the amount of energy transfer to the first harmonic. For the collinear (blue line) and non-collinear (green line) version of the DCTA, with $U_{r,crit}$ = 0.63, even less energy is transferred from the peak to higher frequencies. In contrast to the LTA method, the DCTA method transfers energy to lower frequencies. Within the frequency range 0.2 Hz < f < 0.4 Hz the DCTA variants generate low-frequency energy in the same order as was measured. Decreasing the critical Ursell number to 0.2 again (red line), increases the amount of energy transfer to lower and higher frequencies. We conclude that for the Taman case considered here, SWAN with the DCTA method and $U_{r,crit}$ = 0.63, underestimates the variance density at low frequencies and at the first harmonic. The same conclusion can be drawn for location WHM04 inside the channel. A significant difference with WHM92 is that the variance density at all frequencies is underestimated compared to the measurements for all variants considered. This emphasizes the suspicion of a missing yet unknown mechanism, hampering the wave energy from entering the channel.

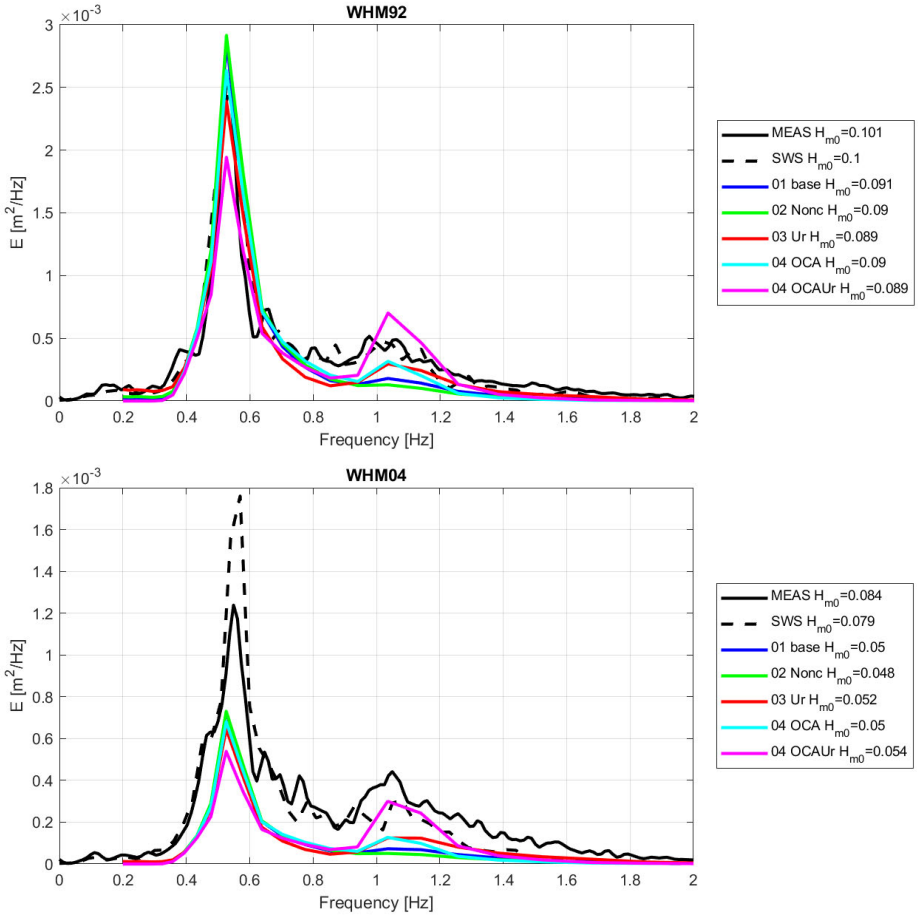

Figure 4.3: Variance density spectra for the Taman case T02 at locations WHM92 (upper panel) and WHM04 (lower panel): observed (black, solid), computed with SWAN for variations (various colors), given in Table 3-1, and SWASH (black, dashed).

If one wants to increase the energy transfer, decreasing the critical Ursell number would be a solution. However, Zijlema (2023) concluded that a critical Ursell number of 0.63 is preferred over 0.2. On the other hand, HKV (2022) concluded that the scaling parameter of the DCTA is extremely sensitive. Since a laboratory case like Taman, as considered here, was not part of the calibration set, a different value might be more appropriate for this test. Increasing the scaling factor $\lambda = 4.4$ by a factor 2 hardly matters, whereas increase to $\lambda = 40$ leads to a more pronounced first harmonic peak and increase of the amount of low-frequency energy. As can be seen from Figure 4.4 this is valid for locations seaward of the channel (e.g. WHM92), inside the channel (e.g. WHM04) and across the channel (not shown). From this test we cannot conclude that the amount of energy transfer to sub- and super-hamonics is sensitive to the changes in the scaling parameter.

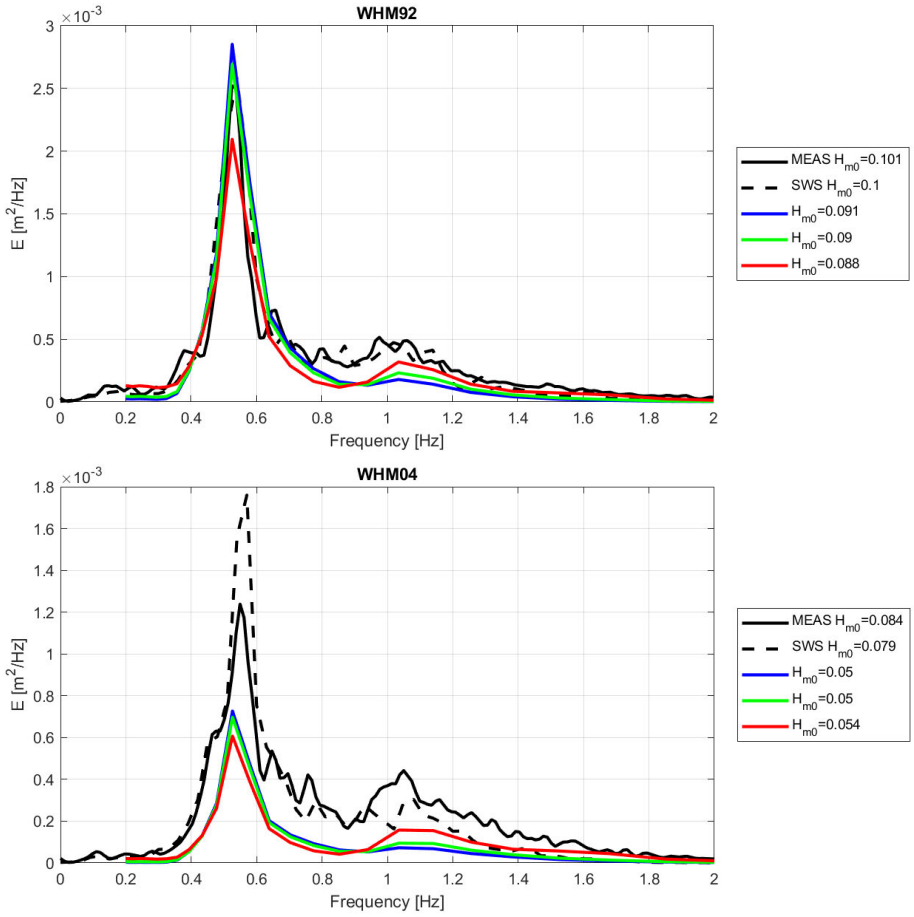

Figure 4.4: Variance density spectra for the Taman case T02 at locations WHM92 and WHM04: observed (black), computed with SWAN for the base case (blue) and with increased scaling parameters: $\lambda = 8.8$ (green) and $\lambda = 40$ (red).

From the comparison of SWAN results, obtained with various triad settings, with both observations and SWASH results we conclude that even the presently implemented non-collinear version of the DCTA formulation cannot avoid the wave energy to be significantly underestimated inside and across the channel. A yet unknown mechanism may be responsible for this underestimation and only increasing the transfer of wave energy to sub- and super

harmonics does not necessarily lead to a better comparison with what is measured or computed with SWASH. Nevertheless, the transfer can be increased by decreasing the default value for the critical Ursell number or increasing the scaling factor significantly.

4.2 Eastern Wadden Sea inlets without wind

4.2.1 Frisian Inlet

For the situation without wind and currents we compare the SWASH and SWAN results in the Frisian Inlet for the November 2007 event. The spatial distribution of the wave height obtained with SWAN with the chosen settings is presented in Figure 4.5. Waves coming from the North break at the ebb-tidal delta between Ameland and Schiermonnikoog and propagate into the Frisian Inlet. Part of the wave energy is clearly dissipated when waves approach the tidal channel in between the islands. The significant wave height south of the channel is in the order of 1 m. Figure 4.6 shows the difference in wave height obtained with SWASH and SWAN. The differences increase up to 1 m on the ebb-tidal delta[1]. Both models have a different concept to model wave breaking. Over the ebb-tidal delta into the inlet the differences between the two models fluctuate. SWASH mostly predicts 0.1-0.2 m higher wave heights. However, in the tidal channel wave heights produced by SWAN are higher. This suggests that blocking of energy by the tidal channel in SWASH is even more pronounced in SWASH than in SWAN.

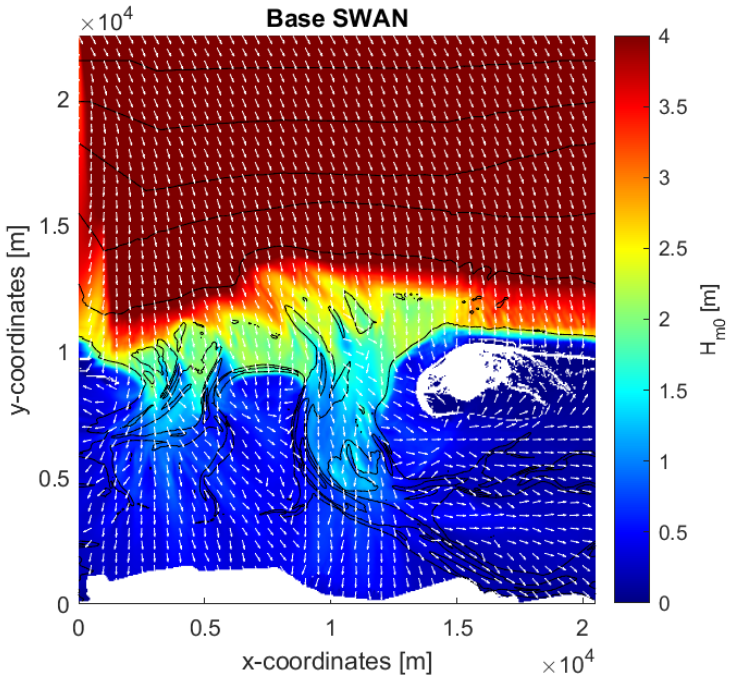

Figure 4.5: Significant wave height in Frisian Inlet, determined with SWAN base settings and without wind and currents. The peak wave direction is shown in white arrows. The black contour lines indicate the bathymetry.

[1] The difference in wave height computed by SWAN and SWASH in the northwestern corner of the domain is more than 1 m, due to the difference in wave boundary condition imposed at the western boundary in SWASH and SWAN.

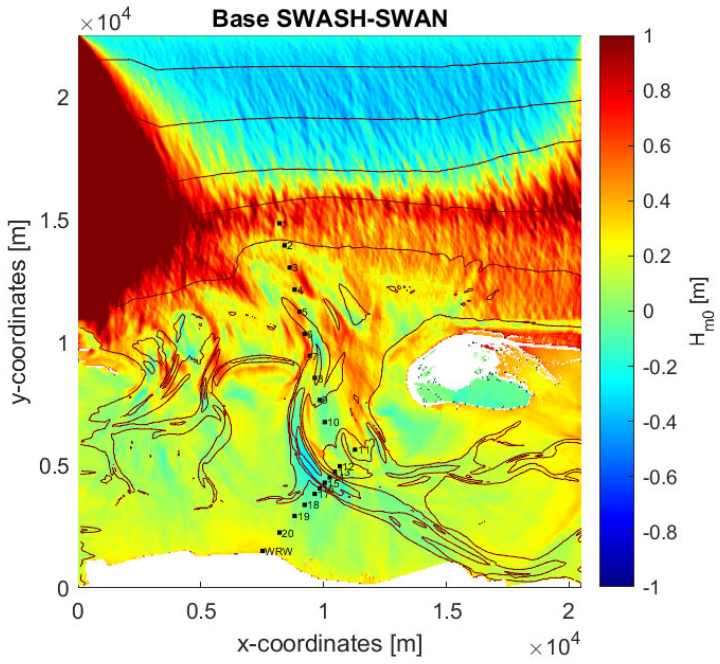

Figure 4.6: Differences in significant wave height between the results, obtained with SWASH and SWAN base settings (without wind and currents) for the Frisian Inlet.

Two rays have been defined, see Figure 4.6 (or Figure 3.3, upper panel for clearer numbering). Figure 4.7 shows the variance densities at the most northern location, which is location 1. Note that for this case the non-collinear DCTA version led to an “unexpected network error”, so results are not available for the non-collinear version for this case. The variance densities obtained with SWAN spectra qualitatively agree with the one obtained with SWASH. The base case predicts a peak at the first harmonic and, as expected, also some energy at the lower frequencies. The LTA method does not generate low-frequency energy. As was observed for the Taman case, lowering the critical Ursell number to 0.2 increases the transfer of energy from the peak to both higher and lower frequencies. The amount of low frequency energy obtained with $U_{r,crit}$ = 0.2 is close to the amount predicted by SWASH at this location.

The DCTA source terms show a smoother evolution over frequencies than the LTA source term. Nevertheless, the DCTA source term with $U_{r,crit}$ = 0.2 shows an unexpected dip near f = 0.14 Hz.

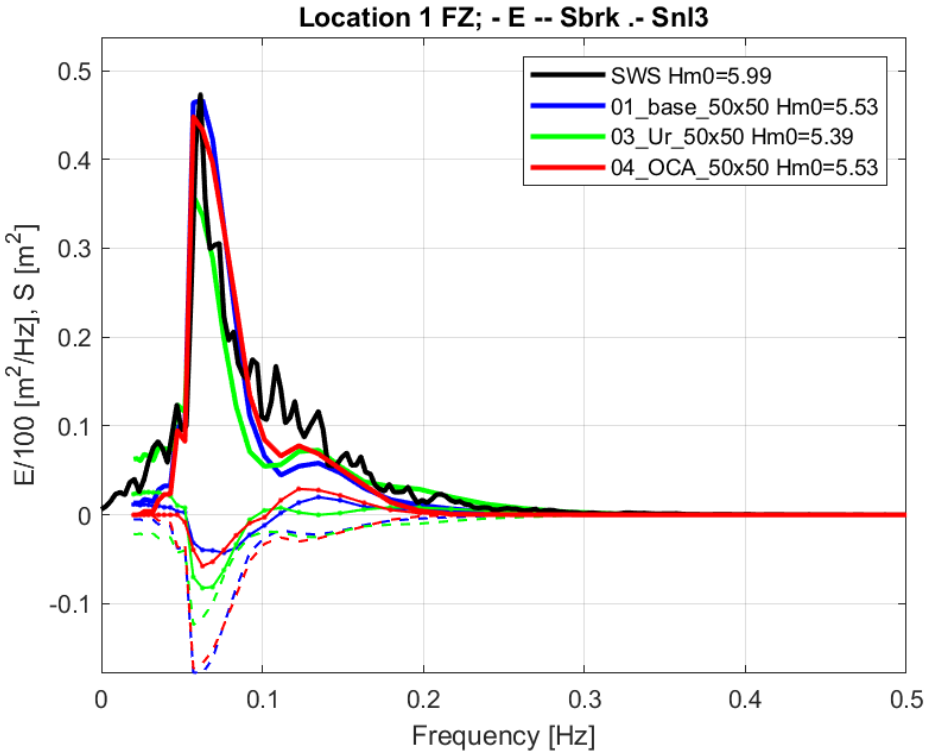

Figure 4.7: Variance density spectra (solid lines) at location 1 of the northern ray in Frisian inlet: SWASH (black) versus SWAN for a variety of settings of the triads: (1) base case (blue), (3) DCTA with $U_{r,crit}$ = 0.2 (green) and (4) LTA with $U_{r,crit}$ = 0.63 (red). Also, the source terms for depth-induced breaking (Sbrk, striped lines) and triads (Snl3, solid dotted lines) have been shown.

Further southward along the northern ray significant differences in spectral shape occur. In Figure 4.8 the variance densities at locations 6 and 9 have been presented. The strongly peaked spectra obtained with the LTA method is not realistic. These peaks are not present when the DCTA method is applied. Low-frequency energy is being generated with the smaller value for $U_{r,crit}$ of 0.2, but maybe too much. The high-frequency tail of the spectrum contains much more energy than being predicted by SWASH. This is possibly caused by the fact that depth-induced breaking in SWAN is not frequency dependent. A stronger dissipation at higher frequencies, being suggested in literature but not (successfully) implemented in SWAN, may have hampered the growth at the tail. The same behavior has been observed along the southern ray, not shown here.

Note the wiggles at the low-frequency part of the spectra. This indicates possible instabilities. Not having wind also means that quadruplets have been deactivated. Normally the quadruplet source term stabilizes the spectral shape. In a computation with wind these instabilities are expected not to occur.

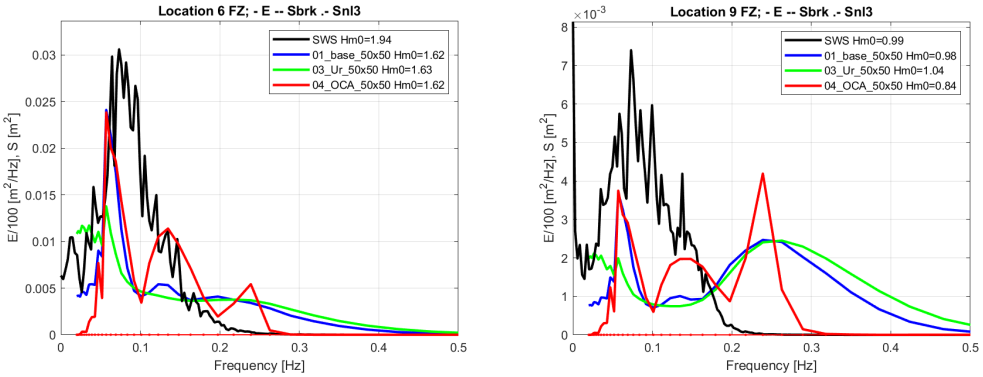

Figure 4.8: As Figure 4.7, but for locations 6 and 9 of the northern ray in Frisian inlet

In Figure 4.9 the variance densities computed with both SWASH and SWAN (base case) at the locations along the southern ray are presented. The same qualitative differences can be observed as for the northern ray. However, most pronounced is the strong decrease in wave energy from location 13 to 14. The SWAN spectra at the locations 13, 14 and 15 and WRW1 are given in Figure 4.10. Where location 13 is on the tidal flat, location 14 is on the edge of the tidal channel (see Figure 3.3). Apparently, the wave energy is partly blocked along the channel edges. The change in wave energy from location 14 to the end of the ray (location WRW1) is much less than the change from location 13 to 14. Not only SWAN but also SWASH shows this behavior. South of location 14 the computed spectra show some variation but not as strong as the jump along the northern bend of the tidal channel.

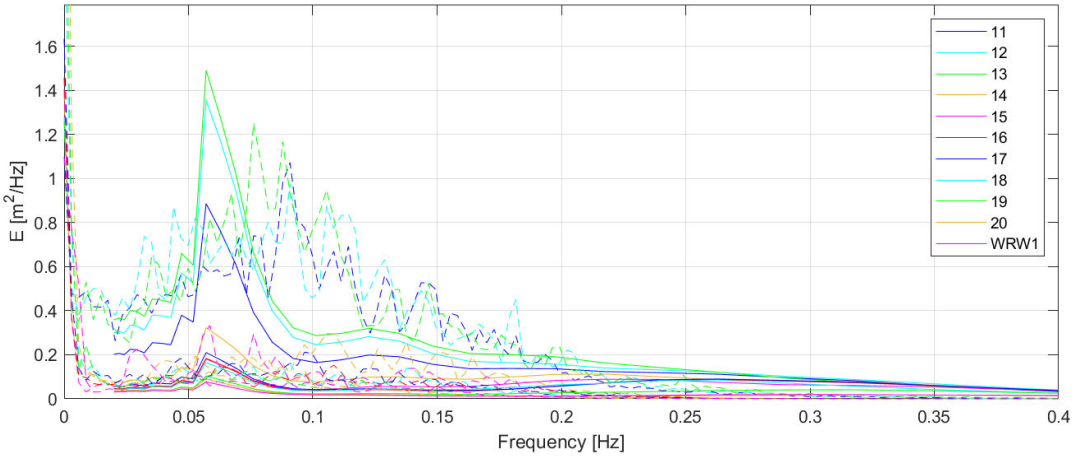

Figure 4.9: Variance density spectra obtained with SWASH (dashed) and SWAN – base case (solid) at output locations along the southern ray in the Frisian Inlet.

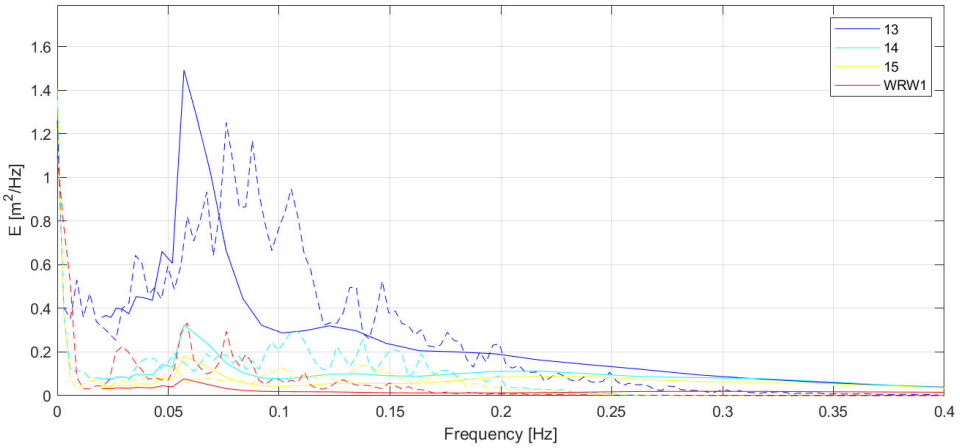

Figure 4.10: Variance density spectra obtained with SWASH and SWAN - base case at output locations 13 (seaward of channel), 14 (edge of channel), 15 (center of channel) and WRW1 in the Frisian Inlet.

4.2.2 Lauwers Inlet

The behavior of the SWAN variants (and SWASH) in the Lauwers Inlet is similar to the Frisian Inlet. Wave energy is clearly blocked at the channel for both SWAN and SWASH, whereas SWASH again shows stronger blocking. In Figure 4.12 the variance density spectra are presented, that are obtained with SWASH and SWAN (four variants, see Table 3-1) at four locations: the most northern location 23 and location 28 south of the channel, both along the northern ray, and location 32 and PBW1 along the southern ray (see Figure 3.3, lower panel, for the numbering of these locations along the rays). The LTA method, with $U_{r,crit}$ = 0.63, again leads to unrealistically peaked spectra, getting more pronounced in southern direction. Both the variance density spectra and the triad source terms obtained with the DCTA method look plausible for as well the collinear as the non-collinear version. Nevertheless, the triad source terms obtained with both versions show a remarkable difference. E.g., at location 28 the source term of the collinear DCTA version (base case) shows a dip at f = 0.14 Hz, whereas the non-collinear version does not. However, more pronounced is the fact that the non-collinear version leads to a triad source term being larger than the one obtained with the collinear version. This should not be possible. The triad source term integrated over frequencies should be zero. This is not true for the non-collinear version, which appears to be +0.001 m^2Hz. We recommend to check the implementation of the non-collinear version of the DCTA method.

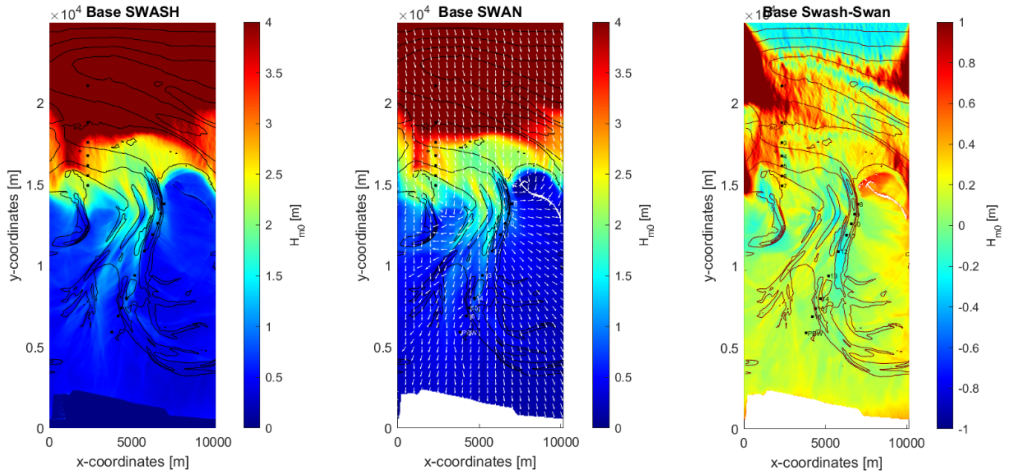

Figure 4.11: Significant wave height in Lauwers Inlet, determined with SWASH (left) and SWAN base settings (middle) and without wind and currents. The peak wave direction is shown in white arrows in the middle figure. The black contour lines indicate the bathymetry. The difference in wave height (SWASH – SWAN) is given in the right panel.

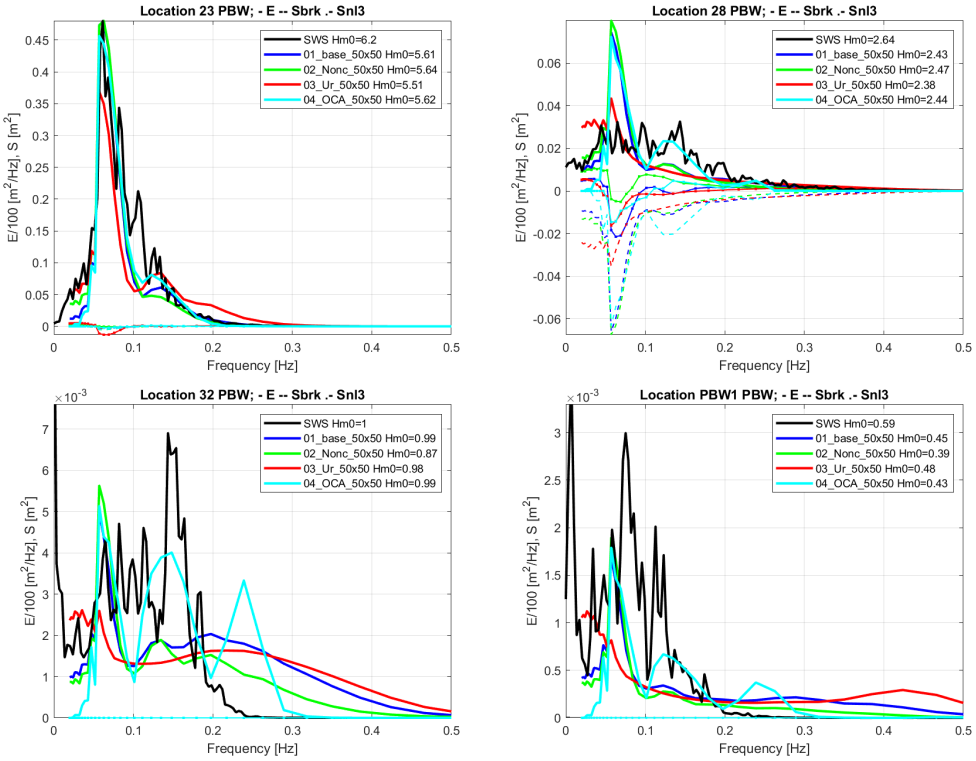

Figure 4.12: Variance density spectra obtained with SWASH (black) and SWAN with different settings (Table 3-1) at locations 23 and 28 along the northern ray and locations 32 and PBW1 along the southern ray in the Lauwers Inlet.

4.3 Eastern Wadden Sea including wind

The storm of 9 November 2007 with north-northwesterly winds has been computed with SWAN. Specifically, case 008 is considered, representing the time instant with the largest significant wave height at wave buoy UHW1. The measured and with SWAN computed variance density spectra are presented in Figure 4.13. The locally generated wind sea peak is predicted correctly for all four SWAN variants. Close to the coast (PBW1, UHW1 and WRW1), the swell peak at $f \approx 0.08$ Hz is significantly underpredicted. To investigate the cause of this underprediction, a closer look at the spectra and source terms along the rays and on spatial maps is taken (elaborated in the remaining of this section). It appears that (low-frequency) energy gets stuck at channel edges and therefore does not propagate throughout the domain, to the wave buoys. This has also been observed in previous section. The hypothesis is that other unknown mechanisms play a role in the accumulation of the low-frequency energy at shallow to deep water edges. This is elaborated in the following of this section.

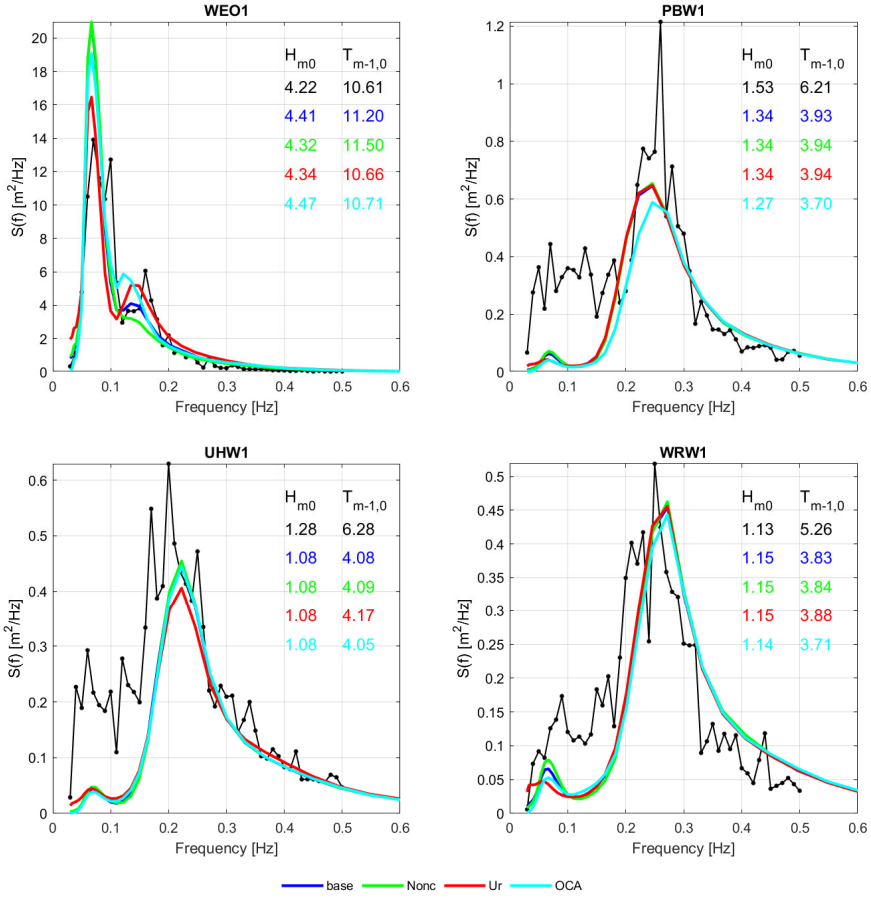

Figure 4.13: Measured and computed variance density spectra with SWAN at four locations. SWAN has been run for a variety of settings of the triads: (1) base case (blue), (2) non-collinear version (green), (3) DCTA with $U_{r,crit}$ = 0.2 (red) and (4) LTA with $U_{r,crit}$ = 0.63 (cyan).

Figure 4.14 shows 1D wave spectra along the three rays close to the coast including the nonlinear wave-wave interactions and wave breaking source terms of the base case. It is noted that all variations (Nonc, Ur and LTA) give a similar picture. The plots show that at some points along the ray, the measured low-frequency energy has been present in the SWAN domain. It seems to be blocked before it reaches the buoys. For the southern ray in the Frisian Inlet (FZ South), for example, it can be seen that a significant amount of low-frequency energy is lost

between location 13 and 14 (see Figure 3.3, upper panel for these locations), also observed for the situation without wind in the previous section. Figure 4.15 shows spatial plots of the significant wave height and wave period zoomed-in to the Frisian Inlet. Overall, it can be seen that energy gets stuck at the right/seaward side of the channel edge. Specifically looking at locations 13 (located outside the channel on a shallow flat) and 14 (inside the deep channel) a significant difference in wave period can be seen. In this case, low-frequency energy cannot move across the channel edge and accumulates at locations 11 through 13.

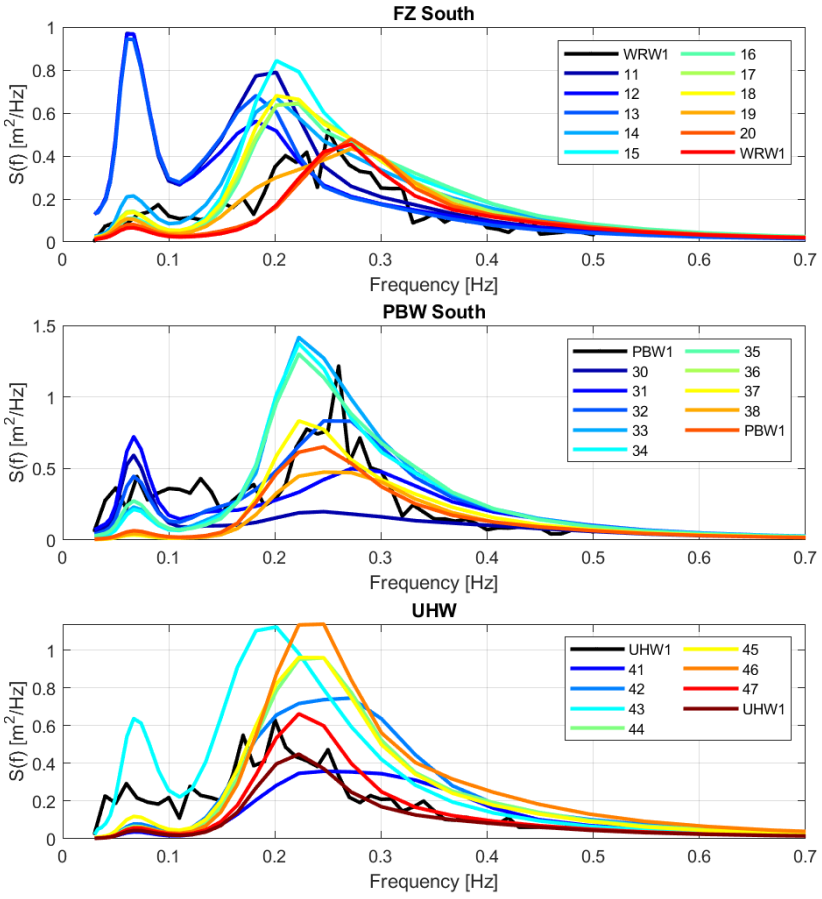

Figure 4.14 Measured (black lines) and computed (base case, colored lines) one-dimensional variance density spectra for the three rays close to the coast in the Eastern Wadden Sea. The locations in the Frisian inlet, Lauwers Inlet and Uithuizerwad are indicated in Figure 3.3 (upper panel), Figure 3.3 (lower panel) and Figure 3.4 respectively.

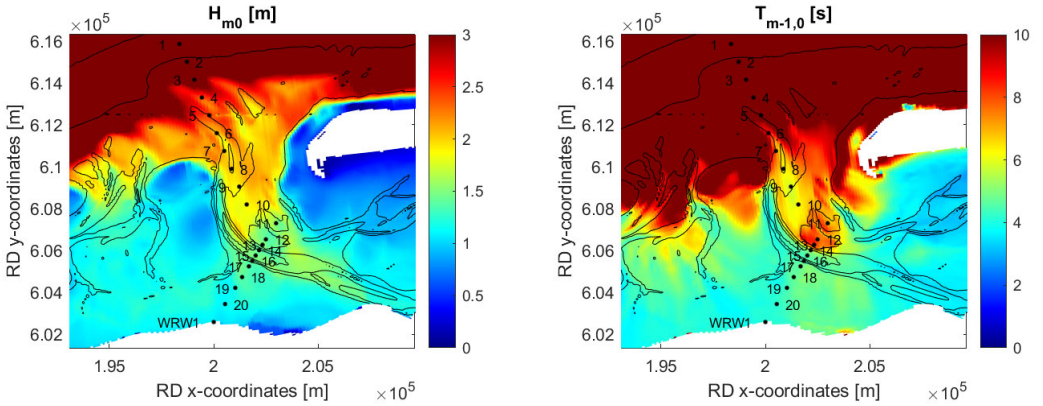

Figure 4.15 Spatial plots of the computed significant wave height (left) and mean wave period (right) for the base case at the Frisian Inlet. The ray output locations are plotted in both figures (even more clearly in Figure 3.3, upper panel).

Figure 4.16 shows the spatial plots of Pieterburenwad. Also here, a similar phenomenon can be observed. Location 29 lies on top of a shallow flat (all locations are clearly indicated in Figure 3.3, lower panel). Moving towards location 31 it can be seen that the wave period suddenly decreases significantly. At this point a deep channel is present. This again shows that low-frequency energy cannot pass a shallow to deep water edge.

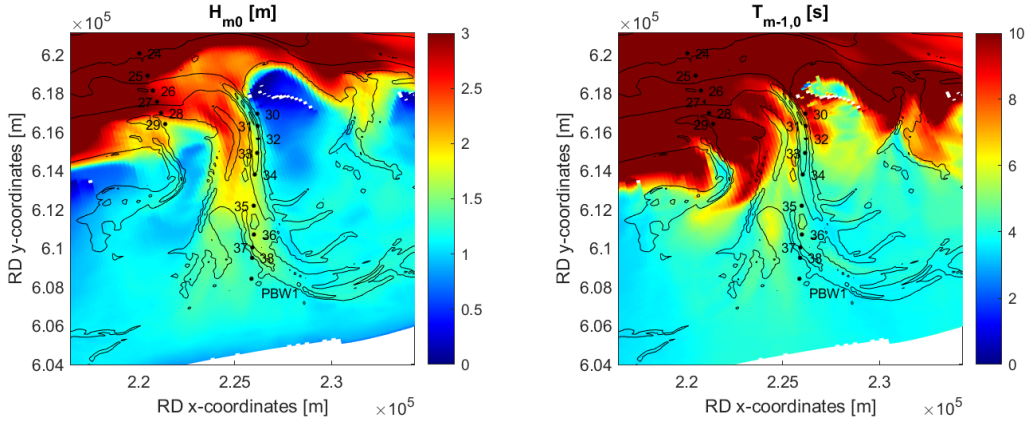

Figure 4.16 Spatial plots of the computed significant wave height (left) and mean wave period (right) for the base case at the Lauwers Inlet. The ray output locations are plotted in both figures (even more clearly in Figure 3.3, lower panel).

For the Uithuizerwad, the wave spectrum at location 43 in Figure 4.14 is remarkable. This is the only location along the ray with a significant amount of low-frequency energy. For all other locations, the low-frequency energy is negligible. Knowing that location 43 lies on top of a shallow flat (see Figure 4.17) and bearing in mind the SWAN computation results at the Frisian and Lauwers Inlet, it makes sense that the wave energy accumulates at the flat of location 43.

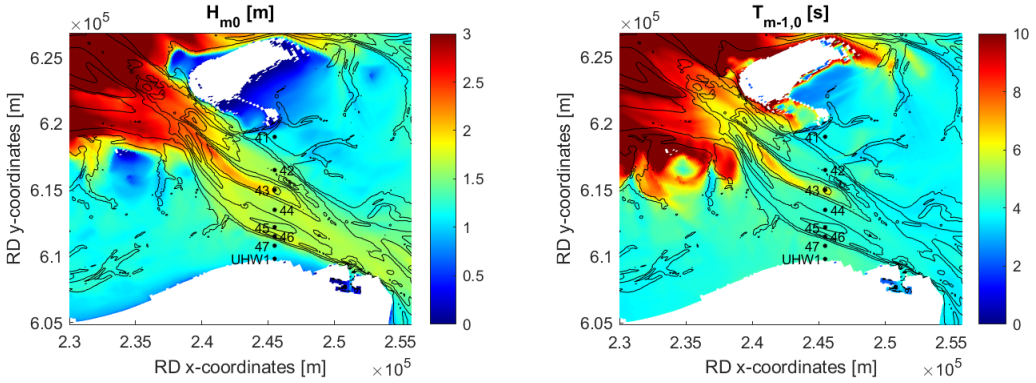

Figure 4.17 Spatial plots of the computed significant wave height (left) and mean wave period (right) for the base case at Uithuizerwad. The ray output locations are plotted in both figures (even more clearly in Figure 3.4).

Concluding, low-frequency energy gets stuck at channel edges and therefore does not propagate throughout the domain, towards the dike. This is not only observed in the SWAN results, but also in the SWASH results, though without wind/currents (Section 4.2.1). The hypothesis is that other mechanisms play a role in the accumulation of the low-frequency energy at shallow to deep water edges. Van der Reijden (2018) suggested that the modelling of refraction in SWAN might be an issue, in combination with the resolution being considered. Besides those mechanisms Rijnsdorp et al. (2021) suggested that wave diffraction, besides nonlinear wave interactions contribute to the wave transmission across the channel, whereas Bragg scattering and wave tunnelling do not. It is noted that decreasing the bottom friction and using the beta-kd breaker model of Salmon and Holthuijsen (2015) results in more low-frequency energy in the SWAN domain, see Figure 4.18. The spatial plots however still show the same behavior as for the other setting variations: at channel edges energy accumulates. Although depth-induced breaking seems to play an important role, further investigation of this mechanism is beyond the scope of this research.

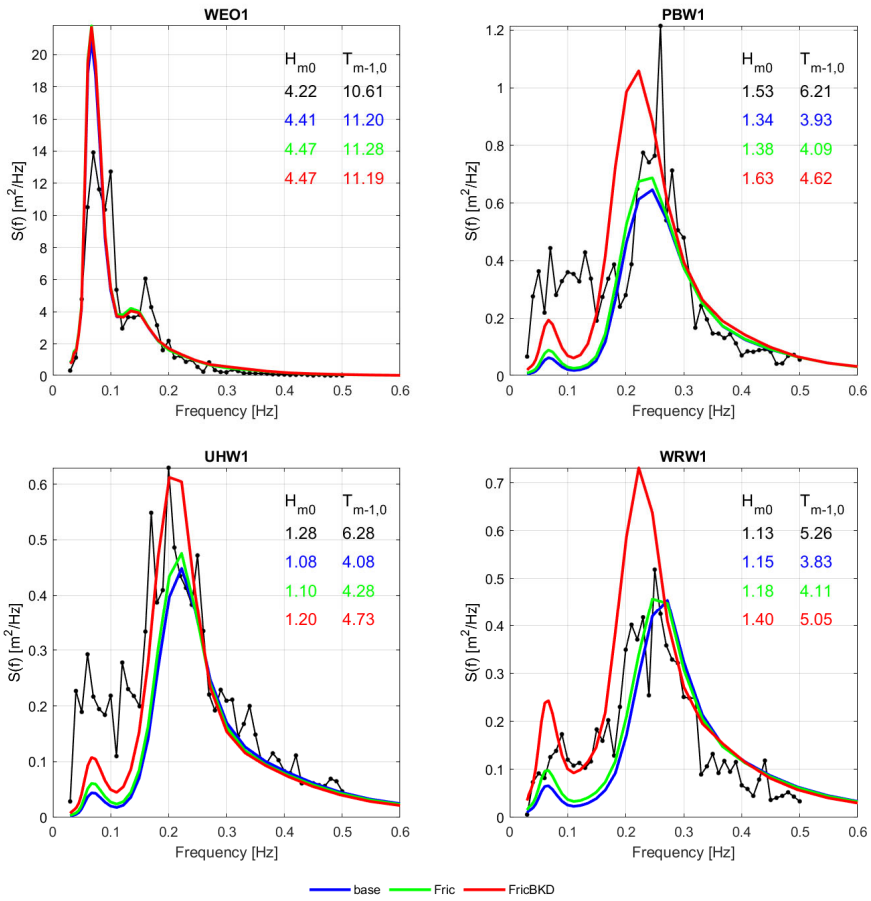

Figure 4.18 Measured and computed variance density spectra with SWAN at four locations. SWAN has been run for a variety of settings: (1) base case (blue), (2) a lower friction coefficient of 0.019 (green) and (3) a lower friction coefficient of 0.019 and beta-kd breaker formulation (red).

4.4 Computational time

Many SWAN computations have been carried out, with both the LTA and DCTA method. For the DCTA method both the collinear and non-collinear version have been applied. Table 4-1 gives an overview of the computational times of the Eastern Wadden Sea SWAN model. Both the total computational time, as well as the time per iteration have been presented. The computations have been performed on the Deltares cluster (virtual Intel Xeon CPU E5-2667 v3 @ 3.20 GHz). It can be seen that the non-collinear version of the DCTA method is significantly more computationally expensive, approximately a factor 60. Therefore, this variant is not (yet) appropriate for practical (BOI or operational) applications. Per iteration the DCTA collinear method is as fast as the LTA method. The latter often leads to a worse convergence behavior.

Table 4-1 Computational times of the Eastern Wadden Sea SWAN model domain including the four nests for the different settings.

Settings	Computational time	No. of iterations	Comp time per iteration
Base	32 minutes	27	0.85 minutes
Nonc	22 hours 10 minutes	27	49 minutes
Ur	33 minutes	28	0.85 minutes
OCA (LTA)	1 hour 4 minutes	80 (max)	0.8 minutes

5 Conclusions and recommendations

In this report the DCTA method for triads is validated, both against a 2D laboratory case (Taman) and a field case (Eastern Wadden Sea). In all cases SWAN results are compared to SWASH results from Rijnsdorp et al. (2021, 2022) and measurements. Various settings for both LTA and DCTA methods have been considered. From the analyses we have drawn various conclusions (Section 5.1) and give a number of recommendations (Section 5.2).

5.1 Conclusions

Conclusions have been drawn related to the DCTA method, as well as related to the penetration of low-frequency energy into the Wadden Sea in general.

5.1.1 DCTA validation

- From a qualitative point of view, the DCTA method seems to be an improvement over the LTA method:
  - The DCTA method transfers energy to lower frequencies, whereas the LTA method by virtue of implementation does not.
  - The shape of the DCTA source term is more realistic, in some cases LTA leads to physically unrealistic peaks in the spectrum.
  - For the Taman case the variance density at the low frequencies and at the first harmonic computed with SWAN does not compare to what is measured or computed with SWASH. The variance density computed with DCTA at these frequency ranges can be increased by decreasing the default value for the critical Ursell number (here from 0.63 to 0.2) or increasing the scaling factor significantly (here from 4.4 to 40). For the field case without wind the DCTA method leads to an overestimation of wave energy at higher frequencies, compared to SWASH results. The LTA formulation leads to nonrealistic spectral shapes, probably due to the omission of quadruplets.
- In the situation without wind, instabilities occurred at the lower-frequency part of the spectrum, for all variants of the DCTA method. The lack of quadruplets, which normally have a stabilizing effect on wave spectra, is probably the reason for this.
- For the Wadden Sea case the DCTA collinear method is as fast as the LTA method per iteration. The computational time of the non-collinear version of the DCTA method is 60 times longer than the collinear version and LTA method. Therefore, it is not appropriate for practical (BOI or operational) applications.

5.1.2 Penetration of low-frequency energy

- For both the laboratory case and the field case (with and without wind/current), wave energy computed by SWAN (with all triad variations) is accumulated near the channel edge. This amount strongly decreases along the rays when crossing the channel edge towards the deeper part of the channel and underestimates the wave energy at the measurement location, at the end of the rays.
- In the field case without wind/currents the strong decrease at the channel edge is observed in both SWASH and SWAN computations, more or less to the same degree, for all variants considered. Another mechanism seems to be responsible for the underestimation of the low-frequency energy at the measurement locations near the Groningen and Frisian coast.
- For the laboratory case SWASH does not show a strong decrease of wave energy at the channel edge. The reason for the difference in SWAN and SWASH behavior is unclear.

- Decreasing the friction coefficient and using the beta-kd breaker formulation led to more wave penetration.

5.2 Recommendations

Based on this study we have the following recommendations:

- Investigate what other mechanism(s) could cause the underestimation of the penetration of North Sea waves into the Wadden Sea. For example, Van der Reijden (2018) refers to the modelling of refraction in SWAN and Rijnsdorp et al. (2021) conclude that diffraction might have a contribution. Depth-limited wave breaking could have contributed as well.
- Since for some cases the LTA method leads to unrealistic shapes of the variance density spectra, whereas the DCTA method does not, consider the DCTA method instead of the LTA method for application in future studies, but only if the following recommendations have been followed up.
- Determine for a large number of testcases the sensitivity of the DCTA method for the scaling parameter λ and critical Ursell number. If the sensitivity appears to be significant, reconsider the DCTA method and underlying assumptions (e.g. bi-phase formulation)) in general and the scaling parameter in particular. .HKV (2022) proved the sensitivity, the present study was not conclusive.
- If the sensitivity is not large, calibrate the DCTA method together with a breaker model suitable for depth-limited situations, using a wide range of tests.
- Check the implementation of the non-collinear version of the DCTA method.

6 References

Alkyon (2009). SWAN hindcast in the Storm of 9 November 2007 Eastern Wadden Sea and Eems-Dollard estuary. Alkyon report A2191, November 2009 (G. Ph. Van Vledder, J. Adema, O.R. Koop).

Battjes, J.A. and J.P.F.M. Janssen (1978). Energy Loss and Set-Up Due to Breaking of Random Waves. 16th International Conference on Coastal Engineering, Hamburg, Germany.

Becq-Girard, F., Forget, P. and Benoit, M. (1999). Non-linear propagation of unidirectional wave fields over varying topography. Coastal Engineering, 38, 91-113.

Beji, S. and J.A. Battjes (1993). Experimental investigation of wave propagation over a bar. Coastal Engineering, 19 (1-2), 151-162.

Boers, M. (1996). Simulation of a Surf Zone with a Barred Beach: Wave heights and wave breaking, Part 1. PhD thesis Delft University of Technology, 116 p.

Booij, N, L.H. Holthuijsen and M. P. Bénit (2009). A Distributed Collinear Triad Approximation in SWAN. Proceedings of Coastal Dynamics 2009, pp. 1-10 (2009). https://doi.org/10.1142/9789814282475_0006.

Deltares (2009). Penetration of North Sea waves into the Wadden Sea. SBW-Waddenzee - phase 3: fallback options. Deltares report 1200114.002, May 2009 (A.R. van Dongeren, A.J. van der Westhuysen, G.Ph. van Vledder, I. Wenneker)

Doering, J.C. and A.J. Bowen (1995). Parametrization of orbital velocity asymmetries of shoaling and breaking waves using bispectral analysis, Coastal Engng., 26, 15-33.

Eldeberky, Y. et Battjes, J. (1995). Parameterisation of triad interactions in wave energy models. Proc. Coastal Dynamics Conference, pp. 140-148

Eldeberky, Y. (1996). Nonlinear transformation of wave spectra in the nearshore zone. Ph.D. thesis, Delft University of Technology, Department of Civil Engineering, The Netherlands.

Groeneweg, J., M. van Gent, J. van Nieuwkoop and Y. Toledo (2015). Wave propagation into coastal systems with complex bathymetries. J. Waterway, Port, Coastal, Ocean Eng., 10.1061/(ASCE)WW.1943-5460.0000300, 04015003

HKV (2022). Modellering laagfrequente golfenergie met SWAN. Aangepaste formulering voor een spectrale bronterm voor triads op basis van de DCTA. HKV rapport PR4658.10, november 2022 (M. Benit).

Komen, G.J., S. Hasselmann and K. Hasselmann (1984). On the existence of a fully developed wind-sea spectrum. J. Phys. Oceanogr., 14, 1271-1285.

Nwogu, O. (1994). Nonlinear evolution of directional wave spectra in shallow water. 24th International Conference on Coastal Engineering, October 23-28, 1994, Kobe, Japan.

Rijnsdorp, D, A. Reniers and M. Zijlema (2021). Verification of SWASH in simulating wave propagation at the scale of a tidal inlet. Delft University interim report, December 2021.

Rijnsdorp, D, A. Reniers and M. Zijlema (2022). Validation phase SWASH - Analysis of swell penetration into tidal inlets and the influence of sea level rise. Delft University report, June 2022.

Salmon, J.E. and L.H. Holthuijsen (2015). Modeling depth-induced wave breaking over complex coastal bathymetries. Coastal Engineering, Vol. 105, 21–35.

Smith, J.M (2004). Shallow-water spectral shapes, Proc. 29th Int. Conf. Coastal Engineering, Lisbon, World Scientific, Singapore: 206-217. https://doi.org/10.1142/9789812701916_0015.

SWAN team (2023). SWAN User Manual. SWAN Cycle III version 41.45.

Van der Reijden, I.M.H. (2018). Modelling refraction of waves over tidal channels. A numerical study focusing on the performance of spectral wave models with respect to bottom refraction. MSc. Thesis Delft University, 136 p.

Van der Westhuysen, A.J. M. Zijlema and J.A. Battjes (2007). Nonlinear saturation based whitecapping dissipation in SWAN for deep and shallow water, Coastal Engng, 54, 151-170.

Zijlema, M. (2023). The role of triad and biphase on the penetration of low-frequency waves in tidal inlets. Memo TU Delft, February 15, 2023.

Deltares is an independent institute for applied research in the field of water and subsurface. Throughout the world, we work on smart solutions for people, environment and society.

Deltares

www.deltares.nl